# Impurity effects on lysozyme crystal growth

**Izumi Yoshizaki,[a*] Akio Kadowaki,[b] Yoshikazu Iimura,[c] Noriyuki Igarashi,[d] Shinichi Yoda[ab] and Hiroshi Komatsu[ae]**

*[a]Space Utilization Research Center, National Space Development agency of Japan, Japan, [b]Department of Innovative and Engineered Materials, Interdisciplinary Graduate School of Science and Engineering, Japan, [c]Advanced Engineering Service, Co. Ltd., Japan, [d]KEK-PF, Japan, and [e]Iwate Prefectural University, Japan. E-mail: yoshizaki.izumi@nasda.go.jp*

We combined Atomic Force Microscopy (AFM) and X-ray diffraction experiment to study the correlation between impurity incorporation, crystal surface morphology and crystal quality. We used Hen Egg White Lysozyme as a model protein, and covalently bound lysozyme dimer as a model impurity. AFM observation of the {101} crystal face revealed that the crystal surface clearly became rough when 5% impurity was added, and the steps disappeared as the impurity concentration increased to 10%. The crystal quality was evaluated by four factors: maximum resolution limit, $\langle I\rangle/\langle \underline{\sigma} I\rangle$, $R_{merge}$, and overall B factor. In every index, the crystal quality tended to degrade as the impurity concentration increased. The B-factor dropped significantly at 5% impurity, at the same time the step roughning was observed. This strongly suggested that the impurity incorporation affected the step growth mechanism and degraded the crystal quality.

**Keywords: protein; lysozyme; impurity; X-ray diffraction; AFM; crystal quality.**

## 1. Introduction

One of the most important factors for growing high-quality protein crystals is the purity of the protein solution. The protein solution contains not only chemical impurities but also physical impurities including aggregates, denatured molecules, structurally related molecules, dust and particles. Removing all impurities similar to the target protein molecule in size and charge is quite difficult because of the limit of the present purification technique. However, these impurities are not a serious problem since most of them can be removed by re-crystallization. Self-impurities such as oligomers cause the serious problems. They are frequently incorporated into the crystal and are thought to degrade the crystal quality (Carter *et al*., 1999, Nakada *et al*., 1999, Caylor *et al*., 1999, Thomas *et al*., 1998, Thomas *et al*., 2000). Carter *et al*. reported that 4.5 times less covalently bound lysozyme dimer (dimer) was incorporated to the crystal, and the resolution improved from 1.6Å to 1.35 Å as a result of microgravity experiment. This report strongly suggested that the impurity incorporation and the crystal quality were strongly correlated. However, the crystal surface morphology was not reported in their paper, so the actual mechanism of quality change were left unclear. Nakada *et al*. actually observed the crystal surface with and without 1% of lysozyme dimer. They found that the {110} face was not sensitive to dimer incorporation, but the {101} face steps became rough in 1% dimer solution. However, no report connected the crystal surface observation and the crystal quality evaluation.

In this study, we studied the correlation between impurity incorporation, crystal surface morphology, and the crystal quality. The crystal surface was evaluated by Atomic Force Microscopy (AFM), and the crystal quality was investigated by X-ray diffraction experiments. In order to investigate the dependence of crystal quality on impurity concentration, we carried out experiments with 0 to 10% of impurity.

## 2. Experiment

### 2.1. Sample preparation

Hen Egg White Lysozyme was used for this experiment. Lysozyme dimer was selected as an impurity. This dimer is formed by covalently bound two lysozyme molecules, and is contained in commercial products (about 0.5% of the commercial lysozyme purchased from Seikagaku Kogyo is dimer). Both lysozyme monomer and dimer had to be highly purified for the quantification of dimer concentration. Therefore, lysozyme monomer was purified to 99.99% purity using the previously reported method (Nakada *et al*., 1999). Dimer was obtained from the commercial lysozyme in four steps. First, the dimer fraction was collected through purification of lysozyme itself. Next, gel filtration chromatography was performed using a G-50 sephadex column ($\phi$2.5×100cm) with 50mM sodium acetate pH 4.5 containing 300mM NaCl. In the third step, gel filtration was repeated for the dimer fraction, which was not sufficiently purified by the first chromatography. Finally, the dimer purity was checked by SDS-PAGE analysis with 10-20% gradient gel. The purity of dimer was determined to be 92.6% from quantification of the band intensity.

### 2.2. AFM observation

Tetragonal lysozyme seed crystals were prepared for AFM observations. Both {101} and {110} surfaces of the seed crystal were used as a substrate to monitor surface morphology in solutions containing various concentrations of dimer. The seed crystals were crystallized by a batch method at 20ºC, in a solution of 75 mg/ml lysozyme, 25 mg/ml NaCl and 50 mM sodium acetate buffer (pH 4.5).

The seed crystals were grown on a glass substrate and set at the bottom of a fluid cell filled with the mother solution. The mother solution in the cell was replaced by the solution containing 0%, 1%, 5% or 10% of dimer two hours before the AFM observation. After the solution in the cell was replaced, the AFM cantilever was approached to the crystal surface for observation.

The observation was performed by contact mode AFM (Seiko Instruments Inc.). The scanner size was 20 $\mu$m × 20 $\mu$m and the spring constant of the $Si_3N_4$ cantilever was 0.09N/m. The scanning rate was 2 to 3 Hz. Different crystals were used for each experiment in order to accurately reflect the surface morphology in each solution.

### 2.3. Crystallization for X-ray diffraction experiment

Tetragonal crystals were grown from the solution of 105mg/ml lysozyme, 25mg/ml NaCl and 50mM sodium acetate (pH 4.5) containing various concentrations of the dimer at 20ºC. The solutions were contaminated with 0%, 2% and 5% of the dimer. Ten percent dimer contaminated crystals were not prepared due to

  

the dimer sample supplement. The crystals were prepared by batch methods.

When the crystals grew to a maximum thickness of 0.2 mm, they were transferred to the synchrotron facility and were subjected to X-ray diffraction study.

### 2.4. X-ray diffraction experiment

Crystals were mounted just before X-ray diffraction data collection. In every case, one crystal was mounted in a 2.0 mm thin-wall glass capillary with the long axis (c axis) of the crystal along the capillary axis. Therefore, the X-ray beam was perpendicular to the c axis. Thus, the thickness of the crystal was regarded to be more important than its length. Since a highly directive X-ray beam was utilized, the illuminated crystal volume could be calculated as 0.1 mm × 0.1 mm (collimator size) × (crystal thickness) mm. Therefore, though the crystals grown in higher impurity concentrations were morphologically shorter, the actual illuminated volume was effectively the same as that of other crystals. The crystal morphology will be described in detail in section 3.2.

Next, we evaluated the crystal quality. The crystals were carefully controlled to the same size to compare the crystal quality without compensation. We collected all data at room temperature using at the BL-6A of the Photon Factory (PF), Tsukuba, Japan. Nearly complete diffraction data sets were collected using an ADSC Quantum 4R CCD detector by the oscillation method with a wavelength of 0.978 Å. Nine samples were analyzed in total. The crystal-to-detector distance was 100 mm in order to obtain adequate reflection separation. The oscillation angle was 1° and the exposure time of 10 seconds per image was constant for all samples.

The X-ray diffraction data were processed in four steps. The images were auto-indexed and integrated using the program *DPS/MOSFLM/CCP4* (Rossman and van Beek, 1999) and then merged and scaled together with *SCALA/CCP4* (Collaborative Computational Project, 1994) using batch scales and smoothing of B-factor. This provided standard crystallographic statistics on crystal quality such as maximum resolution limit, $\langle I \rangle / \langle \underline{\sigma} I \rangle$, overall B factor and $R_{merge}$. The space group was $P4_32_12$, with unit-cell parameters $a = b = 79.1$ (2), $c = 38.0$ (1) Å.

## 3. Results and discussions

### 3.1. Surface morphology

We performed AFM observation to examine the surface morphology in various dimer concentrations.

Figure 1a shows a typical AFM image of a {101} surface of a tetragonal seed crystal in the solution of 75mg/ml lysozyme, 25mg/ml NaCl, 50mM acetate buffer (pH4.5), with no dimer. Figure 1 b shows the {101} surface in the solution with 1% dimer. No significant change was noticed, in contrast to the previous report (Nakada *et al.*, 1999). In a solution containing 5% of dimer, an obvious change was observed. Figure 1c clearly shows that the growth steps roughened, indicating that the dimer affected the step motion pinning the steps. When the 10% dimer was added to the solution, the steps completely disappeared from the surface as shown in Fig. 1d. This means that the dimer molecule was incorporated into and covered the whole surface.

Figure 2 shows the {110} surface of the crystals. No significant change was observed in solutions with 0%, 1% or 5% dimer. With 10% dimer, however, step roughning and the increase of 2D nucleation was observed (Fig. 2d).

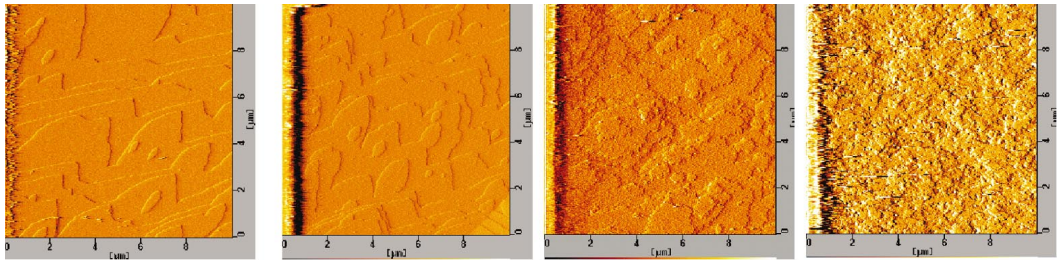

(a) (b) (c) (d)

**Figure 1**

AFM images of {101} surface of tetragonal lysozyme crystal. The images are 10 μm square. (a) The surface with 0% dimer. (b) The surface with 1% dimer. (c) The surface with 5% dimer. (d) The surface with 10% dimer. Note that the surface became rougher as the dimer concentration increased.

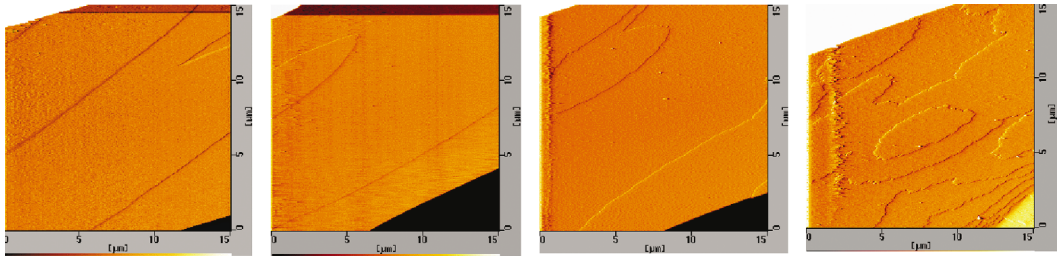

(a) (b) (c) (d)

**Figure 2**

AFM images of {101} surface of tetragonal lysozyme crystal. The images are 10 μm square. (a) The surface with 0% dimer. (b) The surface with 1% dimer. (c) The surface with 5% dimer. (d) The surface with 10% dimer. Note that the surface became rougher as the dimer concentration increased.

### 3.2. Crystal morphology

Crystals for X-ray diffraction experiment were prepared by the method described in section 2.3.

We would like to note that the crystal morphology differed depending on the dimer concentrations. In solutions without the dimer, the aspect ratio of the long side direction length ("L" in Fig. 3) to the short side direction length ("W" in Fig. 3) of the {110} face was 2.3. However, the aspect ratio changed to 1.5 in solutions with 5% dimer. We also measured the crystal growth velocity of each faces by a microscope and revealed that the {101} face growth was suppressed, while the {110} face was not (data not shown). This result is consistent with the AFM observation that showed step roughning in the {101} surface.

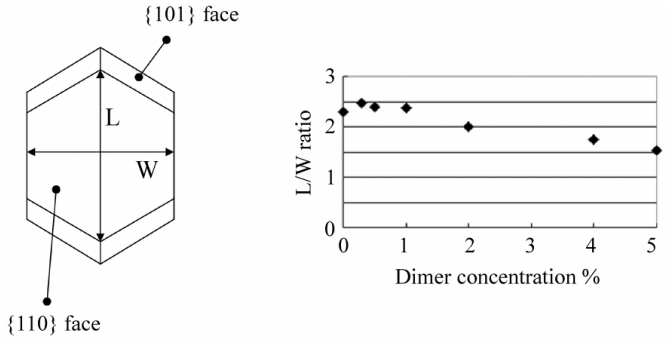


**Figure 3**

Aspect ratio of the crystal grown in various dimer concentrations.

### 3.3. Crystal quality

We evaluated crystals from 0%, 2% and 5% dimer (three crystals for each condition). Intensity data of the crystals showed diffraction up to 1.6 Å to 1.5 Å. The maximum resolution limit was defined as the resolution when $\langle I \rangle / \langle \underline{\sigma} I \rangle$ fell below 2. The worst maximum resolution limit was 1.6 Å. Therefore, in order to compare intensity data with high reliability, only reflections up to 1.6 Å were used for analysis. The data were typically obtained with overall completeness of 96.4% or above, and $R_{merge,}$ below 8%. In the highest resolution shell (1.69 - 1.6Å), completeness was more than 95.9% and $R_{merge}$ was less than 37%. Data multiplicity was 13 - 14 overall, which enabled good statistics. There were approximately 16,100 unique reflections up to 1.6 Å.

The maximum resolution limit, $\langle I \rangle / \langle \underline{\sigma} I \rangle$, $R_{merge}$ and overall B factor are generally accepted criteria for assessing the crystal quality. The maximum resolution limit directly shows the diffracting power of the crystal. If the protein molecules are well packed and aligned, they are expected to diffract well. $\langle I \rangle / \langle \underline{\sigma} I \rangle$ is the signal-to-noise (S/N) ratio of the diffracted intensity where $I$ is the reflection intensity and $\underline{\sigma} I$ is the standard deviation that were obtained by merging symmetry-related reflections. This criterion also reflects the diffracting power of the crystals. $R_{merge}$ is an overall measure of the errors within a dataset. It compares the differences between symmetry-related reflections that should ideally be identical in intensity. The overall B-factor can be calculated from the Wilson Plot in the range of 3 - 1.6 Å. The B-factor difference may reflect thermal vibration, conformational disorder, or static lattice disorders of protein molecules (misorientation). The internal order is expected to be estimated from the B-factor.

The values of these factors for each crystal are summarized in Table 1. Figure 4 shows the B-factor value in each dimer concentration. It is apparent that the B-factor is larger in a higher dimer concentration solution. A close look at Fig. 4 reveals that the crystal quality did not degrade significantly at 2% dimer, but degraded significantly at 5% dimer concentration. This result seems to be consistent with our AFM observation that the crystal surface did not change at 1%, but started roughning at 5% dimer. It is natural to conclude that the dimer molecules incorporated into the crystal caused molecular level disorder, and degraded the crystal quality.

Contrary to our prediction, there were no significant differences in the other three criteria, the maximum resolution limit, $\langle I \rangle / \langle \underline{\sigma} I \rangle$ and $R_{merge}$ (Table1), though there was a tendency for the average value to indicate worse crystal quality at higher dimer concentrations (Fig. 5). The reason is not clear at present, but this may indicate that these criteria are not suitable to detect short range disorders such as small impurity incorporation.

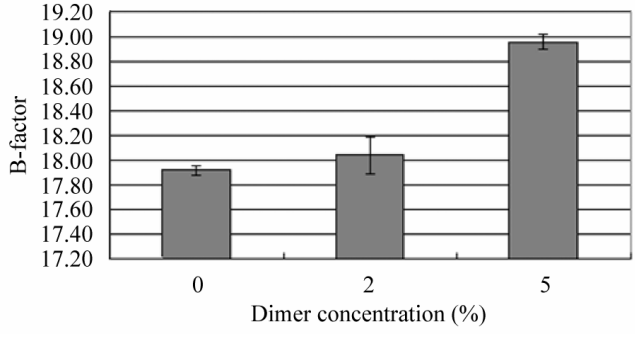


**Figure 4**

B-factor value in various impurity concentration

**Table 1** Crystal data and data collection statistics.

| Sample | a | b | c | d | e | f | g | h | I |
|---|---|---|---|---|---|---|---|---|---|
| Impurity concentration | 0.0 | 0.0 | 0.0 | 2.0 | 2.0 | 2.0 | 5.0 | 5.0 | 5.0 |
| Maximum Resolution limit (Å) | 1.54 | 1.50 | 1.50 | 1.54 | 1.52 | 1.56 | 1.60 | 1.53 | 1.55 |
| Number of unique reflections * | 16377 | 16382 | 15779 | 15895 | 15771 | 16054 | 16279 | 16366 | 16343 |
| Average $<I>/<\sigma(I)>$ * | 8.2 | 8.7 | 10.3 | 9.3 | 9.3 | 9.1 | 6.0 | 8.7 | 8.2 |
| $<I>/<\sigma(I)>$ in the highest resolution shell ** | 2.7 | 3.4 | 3.4 | 2.7 | 3.0 | 2.4 | 2.0 | 3.0 | 2.6 |
| Overall Completeness (%) * | 99.6 | 99.6 | 96.4 | 97.0 | 96.6 | 97.8 | 99.6 | 99.4 | 99.6 |
| Completeness (%) in the highest resolution shell ** | 100.0 | 100.0 | 95.9 | 96.3 | 96.2 | 96.9 | 100.0 | 99.7 | 100.0 |
| Overall $R_{merge}$ (%) # * | 0.054 | 0.048 | 0.043 | 0.052 | 0.049 | 0.053 | 0.073 | 0.049 | 0.055 |
| $R_{merge}$ in the highest resolution shell (%) ** | 0.276 | 0.226 | 0.218 | 0.299 | 0.253 | 0.319 | 0.368 | 0.254 | 0.305 |
| Overall B-factor calculated from the Wilson plot | 17.96 | 17.88 | 17.92 | 18.11 | 17.86 | 18.14 | 18.99 | 18.99 | 18.88 |
| Multiplicity | 13.5 | 13.8 | 14 | 13.6 | 13.8 | 13.5 | 13.8 | 13.3 | 13.3 |
| Unit -cell dimensions (Å) a | 79.10 | 79.16 | 79.12 | 79.18 | 79.03 | 79.24 | 79.02 | 79.19 | 79.05 |
| b | 79.10 | 79.16 | 79.12 | 79.18 | 79.03 | 79.24 | 79.02 | 79.19 | 79.05 |
| c | 37.94 | 37.91 | 37.97 | 37.95 | 37.93 | 37.94 | 37.79 | 37.97 | 37.92 |

* These values were calculated in the range of 10-1.6 Å

** These were the value in the highest resolution shell (1.69-1.6 Å)

# $R_{merge} = \Sigma \mid Ii - < I > \mid / \Sigma Ii$ where $Ii$ is the measured intensity of an individual reflection and $<I>$ is the mean intensity of symmetry - related equivalent reflections.

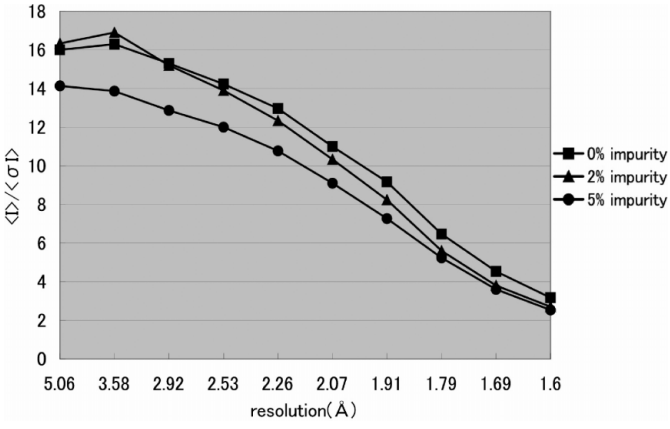


**Figure 5**

Plot showing the mean $<I>/<\sigma I>$ (y axis) versus resolution, $1/d^2=4\sin^2\theta/\lambda^2$ ($Å^{-2}$) (x axis). The average of three crystals for each crystallization conditions is plotted.


### Summary

Lysozyme crystal surface was observed by AFM to study the effect of impurities on crystal surface morphology. 1% of lysozyme dimer did not cause a significant difference, while 5% or more dimer caused serious roughning on the surface. X-ray diffraction experiments were also carried out to evaluate the effect on crystal quality. With 5% impurity, the B-factor indicated significant degradation of crystal quality. We can conclude that the dimer molecules incorporated into the crystal, caused molecular level disorder, and degraded the crystal quality.


We thank the Photon Factory for the beam time allocated for this study (Proposal No. 2001C018).

### References


Carter, D.C., Lim, K., Ho, J.X., Wright, B.S., Twigg, P.D., Miller, T.Y., Chapman, J., Keeling, K., Ruble, J., Vekilov, P.G., Thomas, B.R., Rosenberger, F., Chernov, A.A.: J. Cryst. Growth 196 (1999) 623-637.

Caylor, C.L., Dobrianov, I., Lemay, S.G., Kimmer, C., Kriminski, S., Frnkelstein, K.D., Zipfel, W., Webb, W.W., Thomas, B.R., Chernov, A.A., Thorne, R.E., PROTEINS: Structure, Function, and Genetics 36 (1999) 270-281.

Collaborative Computational Project (1994), Number 4, Acta Cryst. D50, 760-763

Nakada, T., Sazaki, G., Miyashita, S., Durbin, S.D., Komatsu, H.: J. Cryst. Growth 196 (1999) 503-510.

Rossman, M.G., van Beek, C.G. (1999) Acta Cryst. D55, 1631-1640

Thomas, B.R., Carter, D., Rosenberger, F.: J. Cryst. Growth 187 (1998) 499-510.

Thomas, B.R., Chernov, A.A., Vekilov, P.G., Carter, D.C.: J. Cryst. Growth 211 (2000) 149-15